Appl. Phys. A 80, 1745–1751 (2005)
DOI: 10.1007/s00339-003-2471-3

Applied Physics A
Materials Science & Processing

C. CAIZER

Deviations from Bloch law in the case of surfacted nanoparticles

Department of Electricity and Magnetism, Faculty of Physics, West University of Timisoara, Bd. V. Parvan no. 4, 1900 Timisoara, Romania

Received: 13 March 2003/Accepted: 5 November 2003
Published online: 21 January 2004 •

ABSTRACT Bloch's law which describes the variation with temperature of the spontaneous magnetization at low temperatures no longer applies in the case of surfacted nanoparticles. The deviation is a result of the modification of the superexchange interaction in the surface layer of the nanoparticles, which leads to an increase of the magnetic diameter (D_m) (attached to the core where the spins are ferrimagnetically aligned), and of their magnetic moment, when the temperature decreases below 300 K. This anomaly was studied for a ferrofluid containing particles of $Mn_{0.6}Fe_{2.4}O_4$ with a mean physical diameter of $\langle D\rangle = 12.2$ nm that were surfacted with oleic acid. Taking into account the contribution of the layer at the nanoparticles' surface, based on experimental results I have established the law for the variation of the saturation magnetization ($M_{sat}(T)$) with temperature (T) in this case as an addendum to the Bloch law. The temperature dependence of χ_i^{-1} (χ_i – initial susceptibility) of the nanoparticle system in the range $T > T_b$ (T_b – blocking temperature), confirms on the one hand, the increase of the nanoparticles' magnetic diameter when they cool down, and on the other hand, confirms the law that I have found for the dependence $M_{sat}(T)$.

PACS 75.30.Cr; 75.30.Pd; 75.50.Tt

1 Introduction

The saturation magnetization of nanoparticle systems differs significantly from that of the bulk material due to surface effects ('spin canting', 'spin pinning' or 'broken exchange bonds') [1–3] and core-shell morphology. These effects are more intense in ferrimagnetic systems, where the exchange interaction occurs through the oxygen ion O^{2-} (superexchange) [4, 5]. The absence of the oxygen ion at the surface or the presence of another atom (ion) in the form of an impurity leads to a break of the superexchange bonds between the magnetic cations which induce surface spin disorder [3]. Due to the above-mentioned effects, the saturation magnetization in nanoparticle systems is considerably lower than that of bulk ferrite [6, 7]; the decrease is even more pronounced with the increase of the surface-volume ratio of the particle [8].

At low temperatures, the variation of the spontaneous magnetization (M_s) with the temperature (T) is governed by the law in $T^{3/2}$ (the Bloch' law) [9, 10] deduced from the spin wave model

$$M_s(T) = \Gamma(1 - \Lambda T^{3/2}) \tag{1}$$

where Γ is the spontaneous magnetization at 0 K ($M_s(0)$) and Λ is a constant that depends on the exchange integral $J(\Lambda \sim 1/J^{3/2})$. Dependence (1) is well verified experimentally up to room temperature, both for bulk materials (Fe,Ni) [11, 12], and for some spinel ferrites (such as $Mn_xFe_{3-x}O_4$; $0{,}2 < x < 1{,}0$ [13]). Some differences can only be observed for the exponent value of temperature T (e.g. for magnetite the exponent has the approximate value of 2).

In the case of fine particles and clusters, some theoretical calculus and the experimental results have shown that the exponent of the temperature is higher than 3/2 [14–16]. However, Martinez et al. [7] have demonstrated experimentally that in systems made up of γ-Fe_2O_3 nanoparticles with a diameter of $\sim$ 10–15 nm, the saturation magnetization does indeed follow the law in $T^{3/2}$ until room temperature. All these results show that the dependence M_s–T, that was verified for the bulk material does not always apply to systems made up of fine particles and clusters, and there have been various interpretations for this behavior.

Furthermore, when the nanoparticles are covered with oleic acid (organic surfactant), the acid is strongly absorbed on the surface [17] and thus it forms a superficial layer [18]. Here I have studied the variation with temperature of the saturation magnetization of the system composed of surfacted nanoparticles in the temperature range 90–300 K.

It is known that the initial susceptibility χ_i of the nanoparticle system, at zero-field cooling, increases until it reaches its maximum value at the blocking temperature [19]

$$T_b = \frac{KV}{k_B \ln(t_m/\tau_0)} \tag{2}$$

and after that it decreases. In (2), KV is the barrier energy for the magnetic moments of the particles, t_m is the measuring time, τ_0 is the time constant which usually has the value 10^{-9} s, and k_B is the Boltzmann constant. For a fixed measuring time, the position of the maximum in the diagram ($\chi_i - T$) depends on the value of the barrier energy, that is influenced both by the interactions between the particles [20] and by the size distribution of the particles [21]. When no interactions

✉ Fax: +40-256/490-333, E-mail: ccaizer@physics.uvt.ro

are present, for $V = \langle V \rangle$ ($\langle V \rangle$ – mean volume) the nanoparticle system has a superparamagnetic (SPM) behavior in the range $T > T_b$ and a ferrimagnetic (FM) behavior in the range $T < T_b$. In the SPM range, the initial susceptibility varies with temperature according to a Curie-type law for paramagnetic atoms [21]

$$\chi_i(T) = \frac{C_{NP}}{T} \tag{3}$$

where the Curie constant

$$C_{NP} = \frac{\mu_0 n m_p^2}{3k_B} \tag{4}$$

includes the magnetic moment of the particle m_p instead of the atomic magnetic moment. In (4), n is the concentration of the nanoparticles and $\mu_0 = 4\pi \times 10^{-7}$ H/m. When examining the effects of interactions, based on more accurate analysis carried out at temperatures higher than the blocking temperature, it was shown that the variation $\chi_i(T)$ must follow a Curie–Weiss type law [21–24]

$$\chi_{i,NP}(T) = \frac{C_{NP}}{T - \theta} \tag{5}$$

where θ is the ordering temperature resulting from fitting the experimental variation of $1/\chi_{i,NP}$ with temperature to a straight line in a selected range of the temperature [23]. The value of θ is used for indicating the strength of the interactions inside the system, while the sign of θ reflects the type of the interaction that leads to the ordering of the magnetic moments, i.e.(+) for ferromagnetic ordering and (−) for anti-ferromagnetic (ferrimagnetic) ordering. This way, by studying the dependence $1/\chi_{i,NP} - T$ it can obtain additional information concerning the magnetic behavior of the system made up of surfacted nanoparticles at low temperatures.

My research focused on studying the temperature dependence of the saturation magnetization ($M_{sat}(T)$) for ferrimagnetic nanoparticles of $Mn_{0.6}Fe_{2.4}O_4$ that were surfacted with oleic acid and dispersed in kerosene, and establishing the variation law for this case. Additionally, I have analyzed the variation of $1/\chi_{i,NP}$ with temperature for surfacted nanoparticles above the blocking temperature.

2 Experimental

The sample used for the study was a ferrofluid containing $Mn_{0.6}Fe_{2.4}O_4$ nanoparticles that were covered with oleic (organic surfactant) and dispersed in kerosene (solvent), having a concentration of $n = 4.58 \times 10^{22}$ m^{-3} [25]. This way, the stabilisation of the ferrofluid is steric. The polar end of the oleic acid molecule (COO^-) is chemisorbed at the particles' surface [17] (bonds are formed between the free 3d orbitals of the peripheral magnetic ions of the particle, and the electrons from the π orbital of the oleate's carboxyl group, in the structure of the olein molecule). The free part of the molecule (the chain) with a length of $\delta_s \cong 2$ nm is compatible with the (nonpolar) dispersion medium, i.e. the kerosene (the solvent). The nanoparticles were obtained by the chemical co-precipitation method.

Transmission electron microscopy (TEM), of the sample was performed with a JEOL JEM-2010 electron microscope in order to determine the size distribution of the particles.

The magnetic measurements were made with the installation described in [26], that has a data acquisition system (DAQ) connected to a PC. The demagnetising field determined by the sample's geometry $\boldsymbol{H}_d = -N_d \boldsymbol{M}$ (N_d- demagnetising factor) is corrected by a calculation program, so that the magnetization will be recorded as a function of the sample's H field ($H = H_e - H_d$). The experimental installation was calibrated by using Fe and Ni standards. The relative deviation at the measurement of the magnetization is of 1%. During a measurement the relative variation of the magnetic field is of 0.5%. The temperature was measured with a commercial Cu-(Cu/Ni) thermocouple.

The initial susceptibility was measured in the absence of the continuous magnetic field at a frequency (ν) of 50 Hz and an amplitude of the alternating field $H_a = 3$ Oe.

3 Results

The variation of the saturation magnetization of the nanoparticle system in the temperature range 90–300 K is shown in Fig. 1. This was determined from the magnetization curves at saturation, which were recorded both for the sample cooled down from 300 K to 90 K, in the presence of a continuous magnetic field $H_0 = 120$ kA/m applied along the direction where the magnetization will occur, and also in the absence of this field. The continuous magnetic field was applied at room temperature and was maintained at the same value for the whole duration of the cooling and freezing of the sample at 90 K. Following the colloidal system, while returning from 90 K to room temperature, for both the sample cooled in the absence of the continuous field H_0, and in the presence of the field, but only after it has been removed (at 90 K), I have recorded the magnetisation curves at saturation for various values of the temperature. In both cases

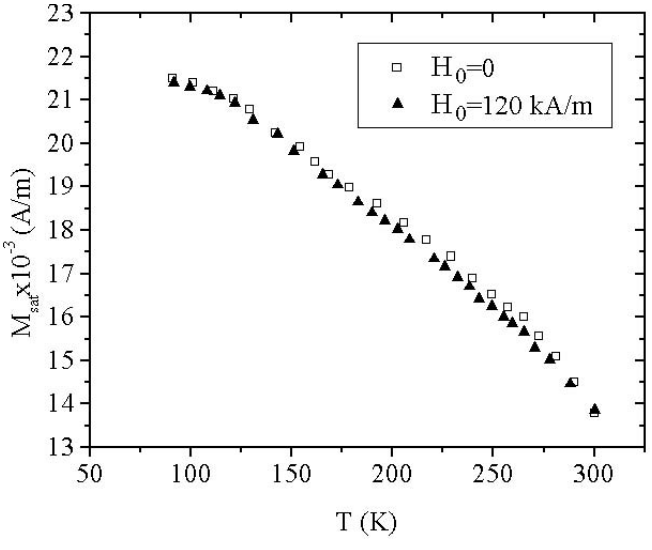

FIGURE 1 Saturation magnetization as a function of temperature of the system composed of $Mn_{0.6}Fe_{2.4}O_4$ nanoparticles surfacted with oleic acid, both in the presence and in the absence of the continuous field H_0

these were then used for determining the saturation magnetization (M_{sat}) that corresponds to a field of 10^5 A/m, and for representing the magnetization M_{sat} as a function of temperature (Fig. 1). Two important aspects can be observed from the diagram: (i) a rapid increase of the saturation magnetization with the decrease of temperature, with a relative variation $\Delta M_{sat}/M_{sat,300} = 55.8\%$ ($\Delta M_{sat} = M_{sat,90} - M_{sat,300}$, the numeric index represents the value of the temperature), that is $\sim 35\%$ higher than the relative variation of the spontaneous magnetization of bulk ferrite ($\Delta M_s/M_{s,300} \cong 21\%$ [10]), in the same temperature range; (ii) the increase of the saturation magnetization does not depend on the fact that the particles, and with them their easy magnetization axes, were oriented (aligned) by the field H_0 along the subsequent measuring direction (in the absence of the field H_0 the easy magnetization axes are randomly oriented from a statistical point of view, with an equal probability of orientation in all directions). This result shows an abnormal increase of the saturation magnetization of the surfacted nanoparticles and this increase is an intrinsic property of the particle.

Additional information regarding the magnetic behavior of the nanoparticle system is provided by the variation of the system's initial susceptibility with the temperature at zero-field cooling (Fig. 2). The maximum of the susceptibility was obtained at a temperature $T_{max} \sim 142$ K. For a particle system where there are no interactions and where there is a size distribution of the particles, in the first approximation $T_{max} \cong \langle T_b \rangle$ ($\langle T_b \rangle$ is the blocking temperature for the same mean volume $\langle V \rangle$) [23, 27]. The blocking temperature is also defined as being the temperature where the measuring time t_m becomes equal to the magnetic relaxation time (τ_m) [28]. In the case of static measurements, $\ln(t_m/\tau_0)$ from (2) has a value of 25 [29]. Formula (2) is still valid for the magnetization in low-frequency harmonic fields (as in my case), but this time $t_m = 1/\nu$ [20], and $\ln(t_m/\tau_0)$ has a value of $16.8 (\nu = 50$ Hz). According to the Néel–Brown relaxation model, the blocking temperature corresponds to the system's transition from the FM state (when $T < T_b$) to the SPM state (when $T > T_b$).

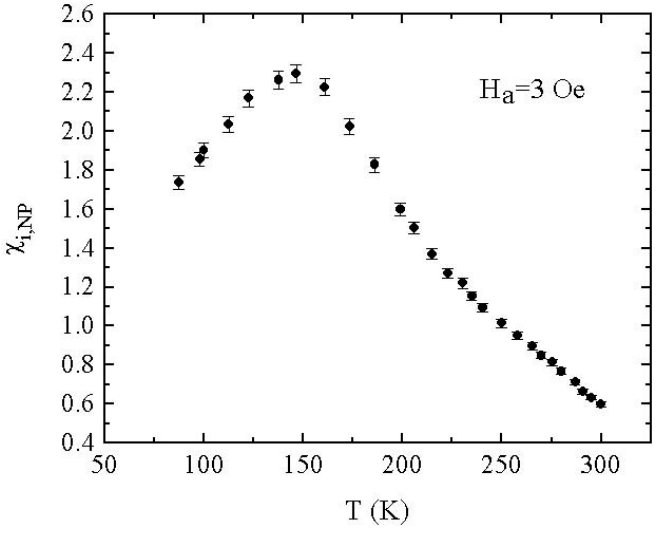

FIGURE 2 Variation of the initial susceptibility with temperature of the system composed of surfacted nanoparticles, recorded at 50 Hz

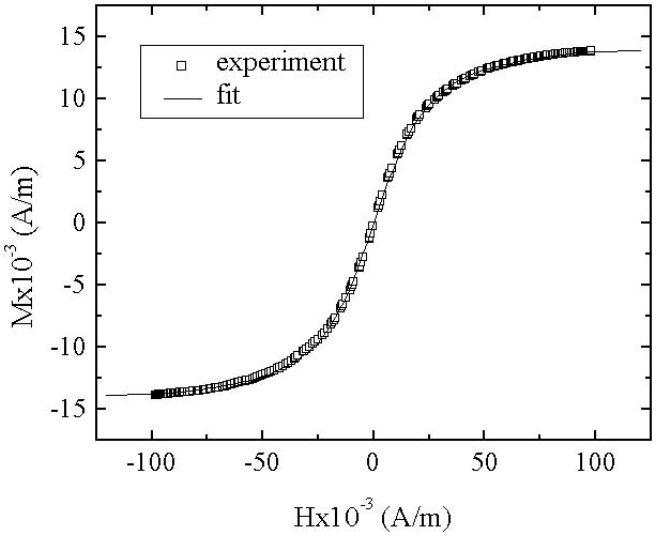

FIGURE 3 M versus H of the sample at 300 K; the continuous line is the fit with the Langevin function

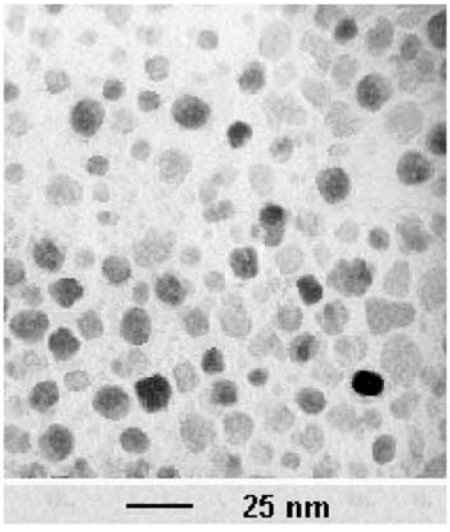

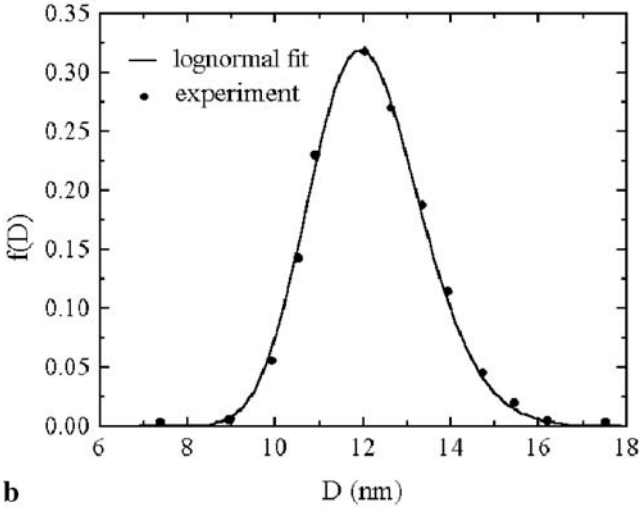

FIGURE 4 **a** Transmission electron micrograph of the sample. **b** Particle diameters distribution in the sample

The magnetization curve of the sample that was recorded at a temperature of 300 K is shown in Fig. 3. The continuous curve in the figure represents the fitting with the Langevin function

$$M(H,T) = M_{\text{sat}}\,[\coth(g\xi) - 1/(g\xi)]\ , \tag{6}$$

where M_{sat} is the saturation magnetization of the ferrofluid, g a parameter that depends on the particles' magnetic moment ($g = \mu_0 m_{\text{p}}/k_{\text{B}}$), and $\xi = H/T$ (H – magnetic field). The overlapping of the theoretical curve (—) with the experimental curve (□) shows that, at room temperature (300 K), the ferrofluid has a superparamagnetic (SPM) behavior. The SPM behavior is also determined by the lack of interactions between the nanoparticles, the magnetic packing fraction $f_m = M_{\text{sat}}/M_{\text{s,300}}$ ($M_{\text{s,300}} = 448 \times 10^3$ A/m [10]) being only 0.0308.

The transmission electron micrograph is shown in Fig. 4a, whereas Fig. 4b shows the distribution of the particles' diameters. After fitting the data (•) with the log-normal function [30]

$$f(D) = (1/\sqrt{2\pi}\delta D)\exp\left\{-\left[\ln(D/D_0)/\sqrt{2}\delta\right]^2\right\} \tag{7}$$

I observe an overlapping between these (solid curve) and the experimental data. The parameters of the distribution are: $D_0 = 12.1$ nm and $\delta = 0.10$. Based on these values, I have determined the mean physical diameter

$$\langle D\rangle = D_0 \exp(\delta^2/2) = 12.2\,\text{nm} \tag{8}$$

of the nanoparticles.

4 Discussion

4.1 *Law for the variation of the saturation magnetization with temperature*

The dependence $M_{\text{sat}}(T)$ both for the $Mn_xFe_{3-x}O_4$ bulk ferrite ($x = 0.6$) (curve α), where $\Gamma = 17.12 \times 10^3$ A/m, $\Lambda = 3.74 \times 10^{-5}\,\text{K}^{-3/2}$ (1) [10] and for the sample made up of nanoparticles that are covered with oleic acid (curve □) (and which was magnetized in the absence of the continuous magnetic field) is shown in Fig. 5. The determined value of the constant Γ was based on the assumption that the saturation magnetization of the nanoparticle would follow the same variation law as bulk material (1) and, at the same time, by taking into consideration the value of the magnetic packing fraction f_{m} ($\Gamma = f_{\text{m}} M_{\text{s}}(0)$, $M_{\text{s}}(0) = 556 \times 10^3$ A/m [31] where $M_{\text{s}}(0)$ is the spontaneous magnetization of at 0 K). In the case of surfacted nanoparticles, I have found that there is a high deviation of the dependence M_{sat} vs. T from curve (α). This difference in behavior was also observed for magnetite nanoparticles covered in oleic acid [26].

This deviation is determined by the increase of the magnetic diameter attached to the nanoparticles' cores where the spins are aligned due to the superexchange interaction. This reasoning is based on our previous results [26] which have shown that the magnetic diameter of the nanoparticles surfacted with oleic acid, increases when the temperature decreases, as it will be shown below for nanoparticles of

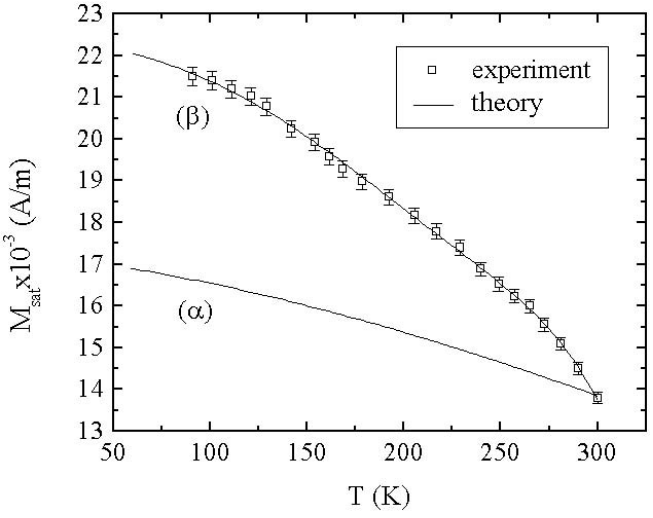

FIGURE 5 *Curves* that represent the dependence of the saturation magnetization on temperature according to (1) (α) and (21) (β); experimental curve (□) in the absence of the continuous field ($H_0 = 0$)

$Mn_{0.6}Fe_{2.4}O_4$. These results led to the idea that the packing fraction f_{m} also increases with temperature, and this aspect has to be taken into consideration when determining the variation of the saturation magnetization with the temperature of the nanoparticle system.

While the saturation magnetization of bulk ferrite is the same as the spontaneous magnetization at 0 K, in the case of ferrofluids it disappears completely since

$$M_{\text{sat}} = f_{\text{m}} M_{\text{s}}\ . \tag{9}$$

Under these circumstances, the magnetic packing fraction of the nanoparticle system at a temperature T

$$f_{\text{m}}(T) = \frac{M_{\text{sat}}(T)}{M_{\text{s}}(T)} \tag{10}$$

and at 0 K, respectively,

$$f_{\text{m}}(0) = \frac{M_{\text{sat}}(0)}{M_{\text{s}}(0)}\ , \tag{11}$$

is not constant anymore (it increases with the decrease of temperature). Furthermore, if in the Bloch law (Eq. (1)) I replace $M_{\text{s}}(T)$ from Eq. (10) and $M_{\text{s}}(0)$ from Eq. (11), I obtain the mathematical expression of the saturation magnetization of the system made up of surfacted nanoparticles

$$\begin{aligned} M_{\text{sat}}(T) &= M_{\text{sat}}(0)\frac{f_{\text{m}}(T)}{f_{\text{m}}(0)}\left(1 - \Lambda T^{3/2}\right) \\ &= M_{\text{s}}(0)\, f_{\text{m}}(T)\left(1 - \Lambda T^{3/2}\right)\ . \end{aligned} \tag{12}$$

In a more restricted form, the temperature dependence of the saturation magnetization of the surfacted nanoparticles system is

$$M_{\text{sat}}(T) = \Gamma(T)(1 - \Lambda T^{3/2})\ , \tag{13}$$

where parameter

$$\Gamma(T) = M_{\text{s}}(0)\, f_{\text{m}}(T) \tag{14}$$

is a function of temperature and not a constant, as in the case of bulk ferrite.

Provided f_m did not depend on temperature and was a constant (the same as the one at room temperature), (12) would be reduced to the Bloch law for bulk material (1), where $\Gamma \equiv M_s(0) = \text{const.}$, and the increase of the saturation magnetization of the system would be a result of the variation of the spontaneous magnetization with temperature.

When f_m is no longer a constant and it depends on temperature (as in my case), a further term has to be included in the equation to reflect this aspect (i.e. the increase of the nanoparticles' magnetic moment and of the magnetic diameter, respectively, with the decrease of temperature); in other words, the law has to be considered as it was written in (12).

Since the saturation magnetization of the nanoparticle system is

$$M_{sat}(T) = nm_p(T) = nV_m(T)M_s(T) \tag{15}$$

in agreement with (10) it results in:

$$f_m(T) = n\pi \langle D_m(T)\rangle^3 /6 \tag{16}$$

(in the approximation of spherical nanoparticles (see Fig. 4a)).

By replacing $f_m(T)$ in (12) I obtain

$$M_{sat}(T) = M_s(0)(n\pi/6)\langle D_m(T)\rangle^3 \left(1 - AT^{3/2}\right) . \tag{17}$$

In (17), $\langle D_m(T)\rangle$ is the mean magnetic diameter of the nanoparticles as a function of temperature. In agreement with (17) it can be concluded that the considerable increase of the saturation magnetization of a system made up of surfacted nanoparticles, compared to that of bulk ferrite, is a result of the increase of the mean magnetic diameter $\langle D_m\rangle$ of the nanoparticles (in which the spins are aligned by means of the superexchange interaction), because $n \cong \text{const.}$ and the increase of the spontaneous magnetization $M_s(T)$ when the temperature decreases from 300 to 77 K (Fig. 5, curve α) is much lower. Our explanation for this behavior is attributed to the modification of the superexchange energy (W_{sch}) in the surface layer of the nanoparticles due to the presence of surfactant molecules [26]. Consequently, the Néel temperature ($T_N \cong W_{sch}/k_B$, k_B – Boltzmann constant) in the superficial layer will change and it will be lower than the room temperature. As the temperature decreases, T_N of the sublayers that are adjacent to the magnetic core of the nanoparticles will be exceeded gradually, so that these sublayers will successively become ferrimagnetically ordered. The result is an increase of the magnetic diameter $\langle D_m\rangle$ attached to the core where the spins are aligned, with the decrease of temperature; this will in turn lead to an increase of the magnetic packing fraction f_m and, implicitly, of the saturation magnetization for the nanoparticle system.

In a different approach, from (15) at temperature T ($T <$ 300 K) and at room temperature I obtain

$$\langle D_m(T)\rangle^3 = \langle D_m\rangle_{300}^3 \left(\frac{M_s}{M_{sat}}\right)_{300} \frac{M_{sat}(T)}{M_s(T)} . \tag{18}$$

The mean magnetic diameter $\langle D_m\rangle_{300}$ at a temperature of 300 K was determined from the magnetization curve (Fig. 3) with the procedure described in [26], admitting a log-normal distribution of the magnetic diameters and the dependence of the particle's magnetic moment on the diameter. In this way, I have found $\langle D_m\rangle_{300} = 10.8$ nm. This value is lower than the mean value of the physical diameter (12.2 nm) that resulted from the TEM, a fact that shows, that in the case of $Mn_{0.6}Fe_{2.4}O_4$ nanoparticles surfacted with oleic acid, a layer is formed on their surface and this layer has an average thickness of

$$\langle \eta\rangle_{300} = (\langle D\rangle - \langle D_m\rangle_{300})/2 = 0.7\ \text{nm} . \tag{19}$$

Replacing in (18) the determined values of $M_{sat}(T)$ [(Fig. 5, (□))], $M_s(T)$ [Fig. 5, curve (α)] and $\langle D_m\rangle_{300}$, I have calculated $\langle D_m(T)\rangle^3$. The resulting values are shown in Fig. 6. According to (19), given that the magnetic diameter increases, the surface layer is narrowing when the temperature decreases (Fig. 6, curve ○). A proof for the fact that the determined values of the diameters $\langle D\rangle$ and $\langle D_m\rangle$ are correct is that at the lowest temperature (90 K), the diameter $\langle D_m\rangle_{90} = 11.9$ nm does not exceed the physical diameter $\langle D\rangle$(12.2 nm). These results show that the layer on the surface of the nanoparticles is paramagnetic at 300 K. As the temperature decreases, the layer gradually becomes magnetically ordered, starting from the core and continuing towards the shell.

Using the electron spin resonance technique, Upadhyay et al. [32] and Sastry et al. [33] have recently shown the existence of the paramagnetic shell of the $Mn_xFe_{1-x}Fe_2O_4$ ($x = 0.1 - 0.7$) nanoparticles in ferrofluid, surfacted with oleic acid. I have highlighted the existence of two absorption lines in the ESR spectrum; one that appears to be due to the ferrimagnetic core, and another one that corresponds to $\varepsilon = 4$, (ε – the spectroscopic splitting factor), attributed to the Fe^{3+} ion in the complex structure made up of oleic acid molecules. The line with $\varepsilon = 4$ disappears at low temperatures. Similarly, Tronc et al. [34] have used Mössbauer spectroscopy at low temperatures to highlight the existence of the paramagnetic layer on the surface of phosphated γ-Fe_2O_3 nanoparticles.

The variation shape of the function $\langle D_m(T)\rangle^3$ in (17) was determined by fitting the experimental values (Fig. 6(●)). The

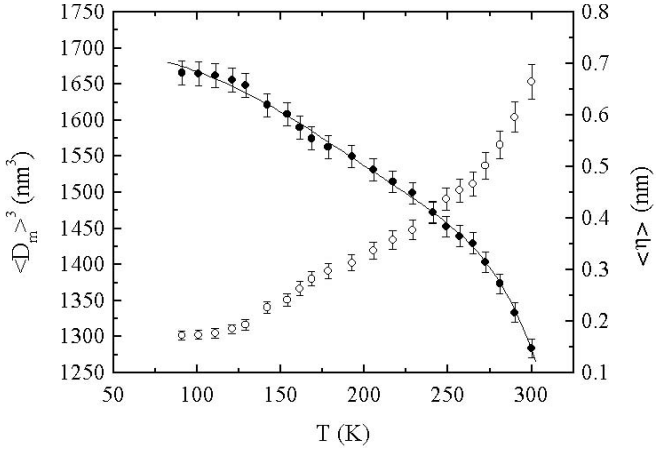

FIGURE 6 $\langle D_m(T)\rangle^3$ vs. T(●) and $\langle\eta\rangle$ vs. T(○) of the nanoparticles; (—) fit curve of $\langle D_m(T)\rangle^3$

variation can be approximated very well with the function

$$\langle D_{\mathrm{m}}(T)\rangle^3 = \sum_{q=0}^{4} c_q T^{2q} \tag{20}$$

(c_q are known constants that were determined from the fit). A good resemblance of the fit curve and the experimental curve can also be obtained if there are two fitting coefficients, however, in order to obtain a more realistic variation of the magnetic diameter with the temperature I have also considered the higher order terms of T^2. The same variation form of $\langle D_{\mathrm{m}}\rangle^3$ with temperature was observed for Fe_3O_4 nanoparticles with a diameter of ~ 11 nm, covered in oleic acid and dispersed in kerosene; however, the fitting coefficients (especially the first two) are different, since they depend on the nature of the material.

Under these circumstances, (17) can be written as

$$M_{\mathrm{sat}}(T) = M_{\mathrm{s}}(0)\frac{n\pi}{6}\left(\sum_{q=0}^{4} c_q T^{2q}\right)\left(1 - \Lambda T^{3/2}\right) . \tag{21}$$

By building the function $M_{\mathrm{sat}} - T$ defined by (21), with the known values of $M_{\mathrm{s}}(0)(556\times 10^3\ \mathrm{A/m})$, $n(4.58\times 10^{22}\ \mathrm{m^{-3}})$, $\Lambda(3.74\times 10^{-5}\ \mathrm{K^{-3/2}})$, and c_q (constants) that resulted from the fit, I have obtained curve (β) in Fig. 5. It can be observed that there is a very good agreement of the calculated curve (—) with the experimental curve (□), which demonstrates that function (21) is suited to describing the temperature variation of the saturation magnetization of the system composed of surfacted nanoparticles. The result obtained demonstrates the accuracy of the function (21), that I have suggested for describing the variation of the saturation magnetization of the surfacted nanoparticle system, with the temperature in a range of low temperatures.

4.2 *The susceptibility*

Knowing the value of the blocking temperature $\langle T_{\mathrm{b}}\rangle$(142 K) from the experimental curve shown in Fig. 2, and using (2) where $V = \langle V_{\mathrm{m}}\rangle_{142} = \pi(\langle D_{\mathrm{m}}\rangle_{142})^3/6$, ($\langle D_{\mathrm{m}}\rangle^3_{142} = 1620\ \mathrm{nm^3}$), and $t_{\mathrm{m}} = 1/\nu = 0.02$ s, I obtain the value of the anisotropy constant $K = 3.9\times 10^4\ \mathrm{J/m^3}$ at a temperature of 142 K. This value is within one order of magnitude higher than the magneto-crystalline anisotropy constant ($|K_{\mathrm{v}}|_{142} \sim 4.5\times 10^3\ \mathrm{J/m^3}$) [35], of $Mn_{0.6}Fe_{2.4}O$ bulk ferrite. Consequently, K has to be seen as an effective anisotropy constant K_{eff}, that also takes into consideration other forms of anisotropy. Since the shape of the nanoparticles is roughly spherical, the shape anisotropy constant (K_{sh}) can't have an order of magnitude higher than $10^3\ \mathrm{J/m^3}$. For this reason, I believe that the surface anisotropy, or more exactly the interface anisotropy (K_{int}), has the most significant contribution to the magnetic anisotropy; this interface anisotropy results from the interaction between the particle and the oleic acid (the iron and manganese ions from the surface of the nanoparticle build bonds with the oxygen ions from the polar end of the oleic acid molecule). This suggests that, in the surface layer of nanoparticles covered in oleic acid, the magnetic moments have a different (disordered) structure compared to that inside the particle, where the spins are ferrimagnetically aligned.

Figure 7 shows the variation with temperature of $1/\chi_{i,\mathrm{NP}}$ for the nanoparticle system. If I calculate the theoretical function $1/\langle\chi_{i,\mathrm{NP}}\rangle$ with (5) where the Curie constant according to Eqs. (4) and (14) is

$$\langle C_{\mathrm{NP}}\rangle_{\mathrm{I}} = \gamma M^2_{\mathrm{s},300}\,\langle D_{\mathrm{m}}\rangle^6_{300} \tag{22}$$

where

$$\gamma = \frac{\mu_0\pi^2 n}{108 k_{\mathrm{B}}} \tag{23}$$

I obtain the straight line (fI) with $\theta = 0$. This line must pass through the experimental value of $1/\chi_{i,\mathrm{NP}}$ at 300 K, because at this temperature the system has a SPM behavior and the interactions are negligible. This case corresponds to the situation when the magnetic diameter does not change with temperature ($\langle D_{\mathrm{m}}\rangle_{300} = 10.8\ \mathrm{nm} = \text{const.1}$) and the variation of the spontaneous magnetization with temperature was neglected ($M_{\mathrm{s}} = M_{\mathrm{s},300} = 448\times 10^3\ \mathrm{A/m} = \text{const.2}$).

However, if I take into consideration the variation of the spontaneous magnetization with temperature, according to (1) the Curie 'constant' becomes

$$\langle C_{\mathrm{NP}}(T)\rangle_{\mathrm{II}} = \frac{\langle C_{\mathrm{NP}}\rangle_{\mathrm{I}}}{M^2_{\mathrm{s},300}}\left[M_{\mathrm{s}}(0)\left(1 - \Lambda T^{3/2}\right)\right]^2 . \tag{24}$$

The function calculated with (5), where the Curie constant is given by (24) and $\theta = 0$, is represented by the curve (fII).

In both cases, it can observe a high deviation of the theoretical curves, (fI) and (fII), from the experimental curve (•).

If apart from the variation of the spontaneous magnetization I also take into consideration the variation of the magnetic diameter, the Curie 'constant' will have the following expres-

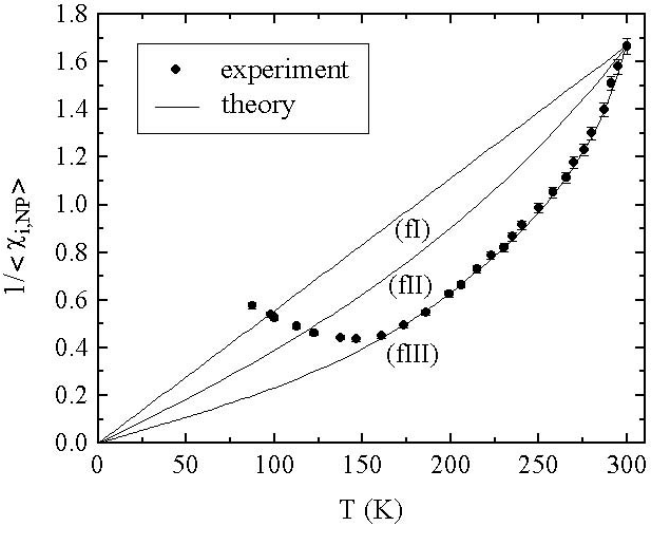

FIGURE 7 Variation of $1/\langle\chi_{i,\mathrm{NP}}\rangle$ with the temperature of the nanoparticle system; (—) curves calculated with (5) and Curie 'constant' with (22) (fI), (24) (fII) and (25) (fIII)

sion:

$$\langle C_{\mathrm{NP}}(T, D_{\mathrm{m}}(T))\rangle_{\mathrm{III}} = \frac{\langle C_{\mathrm{NP}}\rangle_{\mathrm{I}}}{M_{\mathrm{s},300}^2 \langle D_{\mathrm{m}}\rangle_{300}^6} \times \left[M_{\mathrm{s}}(0) \langle D_{\mathrm{m}}(T)\rangle^3 \left(1 - \Lambda T^{3/2}\right)\right]^2 = \frac{\langle C_{\mathrm{NP}}\rangle_{\mathrm{II}}}{\langle D_{\mathrm{m}}\rangle_{300}^6} \left(\sum_{q=0}^{4} c_q T^{2q}\right)^2 . \quad (25)$$

After calculating the corresponding theoretical function, where $\langle D_{\mathrm{m}}(T)\rangle^3$ is given by (20), I obtain the curve (fIII). In the range $T > T_{\mathrm{b}}$, the best overlapping of the calculated curve with the experimental points was obtained for $\theta = -0.4$ K. The value of the temperature θ that is very close to zero shows that the interactions between the nanoparticles can be neglected, a result that is in good agreement with the one deduced from the magnetization curve (Fig. 3) (low magnetic packing fraction; overlapping of the Langevin curve with the experimental curve), and the result deduced from the TEM (Fig. 4a), where it can be seen that the particle clusters are negligible. The sign of θ shows a ferrimagnetic ordering.

On the other hand, the overlapping of the two parts of the theoretical and experimental curves, respectively, in the superparamagnetic range, is another obvious proof – besides the one that resulted from the saturation magnetization – of the increase of the nanoparticles' magnetic diameter with the decrease of temperature. This result confirms the validity of the laws (17), and (21), respectively, which I proposed for the temperature variation of the saturation magnetization at low temperature in the case of surfacted nanoparticles.

5 Conclusions

The saturation magnetization as a function of temperature for the nanoparticles of $Mn_{0.6}Fe_{2.4}O_4$ surfacted with oleic acid is described by the $T^{3/2}$ law $M_{\mathrm{sat}}(T) = \Gamma(T)(1 - \Lambda T^{3/2})$, that contains a parameter that depends on the temperature $\Gamma(T) = M_{\mathrm{s}}(0)(\pi n/6)\langle D_{\mathrm{m}}(T)\rangle^3$, not on the law corresponding to the bulk material, where Γ is a constant ($\Gamma(T) = M_{\mathrm{s}}(0) = \text{const.}$). The variation of the system's saturation magnetization does not depend on the orientation of the easy magnetization axes of the nanoparticles in relation to the magnetization direction, since this is an effect of the material. This anomaly in behavior is a result of the modification of the superexchange interaction in the surface layer of the nanoparticles due to the presence of the surfactant; with the decrease of temperature below 300 K, the superficial layer gradually becomes ferrimagnetically ordered and there is an increase in the volume of the particle core where the spins are aligned. In this way, there will be a secondary effect that is produced by the superficial layer, an effect that is added to the one determined by the nanoparticles' core; these two effects combined determine the deviation from the law $T^{3/2}$ that corresponds to the bulk ferrite. The shape of the function $\Gamma(T)$ depends on the variation of the magnetic diameter with temperature.

The anomaly of the saturation magnetization of nanoparticles surfacted with oleic acid at low temperatures is also confirmed by the variation of $1/\chi_{i,\mathrm{NP}}$ with temperature, above the blocking temperature, which is caused by the increase of the magnetic diameter. C_{NP} from the Curie–Weiss law in the case of surfacted nanoparticles is a function of both temperature and the magnetic diameter: $\langle C_{\mathrm{NP}}(T, D_{\mathrm{m}})\rangle$.

REFERENCES

1 J.M.D. Coey: Phys. Rev. Lett. **27**, 1140 (1971)
2 R.H. Kodama, A.E. Berkowitz, E.J. McNiff Jr., S. Foner: Phys. Rev. Lett. **77**, 394 (1996)
3 A.E. Berkowitz, R.H. Kodama, S.A. Makhlouf, F.T. Parker, F.E. Spada, E.J. McNiff Jr., S. Foner: J. Magn. Mater. **196–197**, 591 (1999)
4 C. Caizer, M. Stefanescu, C. Muntean, I. Hrianca: J. Adv. Mater. **3**, 919 (2001)
5 C. Caizer: Intern. Conf. Adv. Mater. and Structures (AMS 2002), Timisoara (2002); p. 33
6 L. Zhang, G.C. Papaefthymiou, R.F. Ziolo, J.Y. Ying: Nano Structured Mater. **9**, 185 (1997)
7 B. Martinez, A. Roig, X. Obradors, E. Molins, P. Claret, C. Monty: J. Appl. Phys. **79**, 2580 (1996)
8 C. Caizer, M. Stefanescu: J. Phys. D: Appl. Phys. **35**, 3035 (2002)
9 F. Bloch: Zeit. Physik **61**, 206 (1930)
10 A.H. Eschenfelder: In Landolt-Börnstein, *Magnetic properties I* (Springer-Verlag, Berlin 1962) pp. 2–51
11 A.T. Aldred, P.H. Frohle: Int. J. Magnet. **2**, 195 (1972)
12 A.T. Aldred: Phys. Rev. B **11**, 2597 (1975)
13 J.F. Dillon: In Landolt-Börnstein, *Magnetic properties I*, Vol. II(9), Chapt. 29(21), (Springer-Verlag, Berlin 1962) pp. 50–51
14 P.V. Hendriksen, S. Linderoth, P.A. Lindgard: J. Magn. Magn. Mater. **104–107**, 1577 (1992)
15 S. Linderoth, L. Balcells, A. Labarta, J. Tejada, P.V. Hendriksen, S.A. Sethi: J. Magn. Magn. Mater. **124**, 269 (1993)
16 P.V. Hendriksen, S. Linderoth, P.A. Lindgard: Phys. Rev. B **48**, 7259 (1993)
17 C. Rocchicioli-Deltcheff, R. Tranch, V. Cabuil, R. Massart: J. Chem. Res. 126 (1987)
18 R.E. Rosensweig: *Ferrohydrodynamics* (Cambridge Uni. Press, Cambridge 1985)
19 C.P. Bean, L.D. Livingston: J. Appl. Phys. **30**, 120S (1959)
20 J.L. Dormann, L. Spinu, E. Tronc, J.P. Jolivet, F. Lucari, F. D'Orazio, D. Fiorani: J. Magn. Magn. Mater. **183**, L255 (1998)
21 G. Gittleman, B. Abelas, S. Bozowski: Phys. Rev. B **9**, 3891 (1974)
22 F. Söffge, E. Schmidbauer: J. Magn. Magn. Mater. **24**, 54 (1981)
23 K. O'Grady, M. El-Hilo, R.W. Chantrell: IEEE Trans. Magn. **29**, 2608 (1993)
24 C. Cannas, D. Gatteschi, A. Musinu, G. Piccaluga, C. Sangregorio: J. Phys. Chem. B **102**, 7721 (1998)
25 C. Caizer: Solid State Commun. **124**, 53 (2002)
26 I. Hrianca, C. Caizer, Z. Schlett: J. Appl. Phys. **92**, 2125 (2002)
27 J.L. Dormann, F. D'Orazio, F. Lucari, E. Tronc, P. Prené, J.P. Jolivet, D. Fiorani, R. Cherkaoui, M. Nogués: Phys. Rev. B **53**, 14 291 (1996)
28 L. Neel: Adv. Phys. **4**, 191 (1955)
29 H. Mamiya, I. Nakatani: J. Appl. Phys. **81**, 4733 (1997)
30 J.C. Bacri, R. Perzinski, D. Salin, V. Cabuil, R. Massart: J. Magn. Magn. Mater. **62**, 36 (1986)
31 A.H. Eschenfelder: J. Appl. Phys. **29**, 378 (1958)
32 R.V. Upadhyay, D. Srinivas, R.V. Mehta: J. Magn. Magn. Mater. **214**, 105 (2000)
33 M.D. Sastry, Y. Babu, P.S. Goyal, R.V. Mehta, R.V. Upadhyay, D. Srinivas: J. Magn. Magn. Mater. **149**, 64 (1995)
34 E. Tronc, A. Ezzir, R. Cherkaoui, C. Chanéac, M. Noguès, H. Kachkachi, D. Fiorani, A.M. Testa, J.M. Grenèche, J.P. Jolivet: J. Magn. Magn. Mater. **221**, 63 (2000)
35 R.F. Penoyer, M.W. Shafer: J. Appl. Phys. **30**, 315S (1959)